Title: Associations between COVID-19 and putative markers of neuroinflammation: A diffusion basis spectrum imaging study.

Wei Zhang [a,#], Aaron J Gorelik [b], Qing Wang [a], Sara A Norton [b], Tamara Hershey [a,b,c,d], Arpana Agrawal [c], Janine D Bijsterbosch [a,#,*], Ryan Bogdan [b,*]

[a] Mallinckrodt Institute of Radiology, Washington University School of Medicine, St. Louis, MO, United States
[b] Department of Psychological & Brain Sciences, Washington University, St. Louis, MO, United States
[c] Department of Psychiatry, Washington University School of Medicine, St. Louis, MO, United States
[d] Department of Neurology, Washington University School of Medicine, St. Louis, MO, United States

[#] Corresponding authors
[*] Shared senior authorship

Corresponding Authors:

Full name: Wei Zhang; Janine Bijsterbosch

Department: Radiology

Institute/University/Hospital: Washington University School of Medicine, St. Louis

Street Name & Number: 4525 Scott Ave.

City, State, Postal code, Country: St. Louis, MO 63110, USA

Tel: 314-629-3344

E-mail: weiz@wustl.edu; Janine.bijsterbosch@wustl.edu

Abstract (word count: 249)

COVID-19 remains a significant international public health concern. Yet, the mechanisms through which symptomatology emerges remain poorly understood. While SARS-CoV-2 infection may induce prolonged inflammation within the central nervous system, the evidence primarily stems from limited small-scale case investigations. To address this gap, our study capitalized on longitudinal UK Biobank neuroimaging data acquired prior to and following COVID-19 testing (N=416 including n=224 COVID-19 cases; M_{age}=58.6). Putative neuroinflammation was assessed in gray matter structures and white matter tracts using non-invasive Diffusion Basis Spectrum Imaging (DBSI), which estimates inflammation-related cellularity (DBSI-restricted fraction; DBSI-RF) and vasogenic edema (DBSI-hindered fraction; DBSI-HF).We hypothesized that COVID-19 case status would be associated with increases in DBSI markers after accounting for potential confound (age, sex, race, body mass index, smoking frequency, and data acquisition interval) and multiple testing.

COVID-19 case status was not significantly associated with DBSI-RF (|β|'s<0.28, p_{FDR} >0.05), but with greater DBSI-HF in left pre- and post-central gyri and right middle frontal gyrus (β's>0.3, all p_{FDR}=0.03). Intriguingly, the brain areas exhibiting increased putative vasogenic edema had previously been linked to COVID-19-related functional and structural alterations, whereas brain regions displaying subtle differences in cellularity between COVID-19 cases and controls included regions within or functionally connected to the olfactory network, which has been implicated in COVID-19 psychopathology.

Nevertheless, our study might not have captured acute and transitory neuroinflammatory effects linked to SARS-CoV-2 infection, possibly due to symptom resolution before the imaging scan. Future research is warranted to explore the potential time- and symptom-dependent neuroinflammatory relationship with COVID-19.

Keywords: Neuroinflammation, COVID-19, Long COVID, UK Biobank, neuroimaging, Diffusion Basis Spectrum Imaging, DBSI.

Introduction (word count = 1069)

The ongoing COVID-19 pandemic remains a threat to global health and economies. In America alone, at least 42% of adults have been diagnosed with COVID-19 during their lifetime (1), and approximately 20% of them experience longer-term consequences, collectively referred to as long-COVID (2). These consequences include issues like loss of smell, psychopathology symptoms (e.g., sleep disorders, depression, anxiety), fatigue, cognitive impairment (also known as “brain fog”), and increased mortality (3–6). Concurrently, the pandemic continues to impose a substantial worldwide economic burden (7). Within the United Sates, the total estimated economic toll surged to $3.7 trillion USD in 2022 (8), up from the initial projections of $2.6 trillion USD (9). This encompasses expenses tied to diminished quality of life, decreased earnings, and escalated medical costs stemming from the long-lasting effects of COVID-19 (10,11). These persistent challenges underscore the vital need for a comprehensive understanding of the underlying mechanisms through which COVID-19 impacts both health and behavior.

Accumulating evidence suggests that COVID-19 may have a profound impact on brain structure (6,12–14). Specifically, neurological events associated with COVID-19 such as stroke, vascular thrombosis, and microbleeds have been located throughout both cortical and deep subcortical structures (15), and individuals with SARS-Cov-2 infection have shown both cross-sectional and longitudinal changes in grey matter and white matter areas that are associated with cognitive impairment, sensory abnormalities, and mental health issues even months after the first infection (13,14). For example, a recent study using longitudinal imaging data acquired prior to and following COVID-19 testing (total N=785 including n=401 COVID-19 cases), found reductions in cortical thickness and volume for individuals with a COVID-19 diagnosis in the orbitofrontal cortex and related regions (e.g., piriform cortex) that are involved in the olfactory network (16). Notably, these COVID-19 related longitudinal brain structure changes were also observed in individuals who had not been hospitalized (16). Evidence showing the association between COVID-19-related brain structural alterations and impaired cognitive performance further suggests that some COVID-19 related symptomatology may be attributable to changes in brain structure (21) and linked to elevated inflammation in the brain (22,23). Interestingly, these brain-behavior associations may not resolve with time since COVID-19 related differences in brain structure have been observed one- and two-years following hospitalization (24,25).

To elucidate the potential mechanisms contributing to these COVID-19-related structural changes in the brain, it becomes crucial to delve into the inflammatory processes in the central nervous system (26,27). SARS-CoV-2 infection leads to activation of inflammatory signaling cascades, which can become dysregulated resulting in excessively high inflammation, known as cytokine storms (28–30). This hyperactivity of the immune system can disrupt the blood-brain barrier (31), enabling peripheral inflammatory markers to gain access into the CNS, which can directly increase neuroinflammation and may then impact brain structure (32). As such, neuroinflammation may occur in COVID-19 patients at the acute phase of disease (33–35) and persist in long-COVID patients with neuropsychiatric symptoms (22,36). Brain olfactory regions may be particularly vulnerable to these hyperactive responses. For example, a study of golden hamsters found that SARS-CoV-2 infection may increase microglial and infiltrating macrophage activation in olfactory tissues, which was associated with behavioral alterations in scent-based food finding (37). Further evidence comes from post-mortem data in human COVID-19 patients and a rhesus macaque model of COVID-19 showing inflammation in the blood-brain barrier (i.e., choroid plexus; (38)), T-cell infiltration, and microglia activation (39).

While still in its preliminary stages, few positron emission tomography (PET) case studies have provided *in vivo* data establishing a connection between COVID-19 and neuroinflammation. These studies have demonstrated widespread increases in [^{18}F]DPA-714

binding throughout the brain in two long-COVID patients (36), higher levels of translocator protein (TSPO) in the brainstem that were correlated with the clinical progression of one patient who had experienced both COVID-19 vaccination and subsequent infection (40). Additionally, elevated translocator protein distribution volume (TSPO V_T) was observed in 20 participants who continued to suffer from persistent depressive and cognitive symptoms after initially experiencing mild to moderate SARS-CoV-2 infection (22). However, as of now, there have yet to be any large-scale investigations of neuroinflammation in the context of COVID-19.

Here, we tested whether COVID-19 is associated with changes in putative neuroinflammation in a cohort of N=416 individuals (n=244 infected cases and n=192 non-infected controls) from the "COVID-19 repeat imaging" sub-study of the UK Biobank (41). This sub-study collected neuroimaging data from individuals prior to and following a COVID-19 positive or negative test (e.g., based on diagnoses comprising PCR test, hospital impatient admission or GP records, as well as home-based test; see details in source of positive test result below in Methods). Neuroinflammation was assessed with putative markers of neuroinflammation-related cellularity and vasogenic edema. These markers were derived from diffusion-weighted imaging data, employing the Diffusion Basis Spectrum Imaging (DBSI) technique.

DBSI is an extension of standard Diffusion Tensor Imaging (DTI). While DTI focuses solely on estimating direction-dependent water movement parameters through anisotropic tensors, DBSI represents the diffusion-weighted imaging signal with multiple anisotropic and isotropic tensors (42–44). More importantly, the DBSI approach provides a spectrum of isotropic diffusion metrics, including restricted fraction (DBSI-RF), which indicates inflammation-related cellularity –either from cell proliferation or infiltration. Higher values of DBSI-RF suggest higher levels of inflammatory cell fraction. DBSI-RF as a putative neuroinflammation marker has been validated in a series of experiments. It demonstrated associations with inflammation-related cellularity derived from immunohistochemistry in an experimental mouse model of induced autoimmune encephalomyelitis (44), and with stain-quantitated nuclei and microglia density (i.e., cellularity) from post-mortem human brain tissues (45). Higher levels of DBSI-RF have also been linked to inflammation-related conditions, including multiple sclerosis (43,46–48), obesity (49,50), HIV (51), Alzheimer's disease (45,49,52), and depression (49), as well as markers of disease progression (45,54). In addition to DBSI-RF, hindered fraction from the DBSI estimation (DBSI-HF) has shown promise as a putative marker for indicating inflammation-related cerebral edema (43,55), and has been linked to inflammatory conditions including obesity (49,50), and Alzheimer Disease (52). Nevertheless, both DBSI-RF and DBSI-HF as proposed markers of neuroinflammation would benefit from more validation work in these condition to which it is applied.

Here, employing this novel and non-invasive approach to assess neuroinflammation, we hypothesized that SARS-CoV-2 infection would be associated with increases in DBSI neuroinflammation markers across the brain with the most profound differences in brain regions that showed the strongest COVID-19 related structural changes (e.g., orbitofrontal cortex, piriform cortex) in the human brain (20)) or neuroinflammatory changes (e.g., microglia activation in olfactory bulb) in post-mortem or animal studies (37,39,56).

Materials and Methods (word count = 1, 640)

Sample.

The UK Biobank (UKB) is a large-scale study (N > 500,000 participants) designed to examine the genetic, environmental, biological, and behavioral correlates of broad-spectrum health outcomes and related phenotypes (58). In February 2021, a UKB sub-study, the 'COVID-19 repeat imaging study,' was launched to collect neuroimaging data at a second timepoint, following either a positive (cases) or negative (controls) COVID-19 test, among individuals who completed a neuroimaging session prior to the COVID-19 pandemic to study longitudinal neuroimaging correlates of SARS-CoV-2 infection. COVID-19 positivity/negativity prior to the second neuroimaging session was determined from 3 sources: 1) hospital records contained in the Hospital Episode Statistics (a database containing admissions, outpatient appointments, and attendances and emergency admissions to English National Health Service Hospitals), or 2) primary care (GP) data, and 3) a record of a positive COVID-19 antibody test obtained from a home-based lateral flow kit sent to participants. For individuals who completed home testing and were vaccinated, a second testing kit was collected to ensure that any antibodies detected were from infection as opposed to recent vaccination (20). Participants were identified as COVID-19 positive cases if they had a positive test record on any of these data sources. COVID-19 negative participants (i.e., controls) were then selected in this sub-study from the remaining participants that were previously imaged before the pandemic to achieve 1:1 matching to the COVID-19 positive cases on sex, race (white/non-white), age (date of birth), location and date of the first imaging assessment. Details of inclusion criteria and case-control matching are provided in online documentation (https://biobank.ndph.ox.ac.uk/showcase/showcase/docs/casecontrol_covidimaging.pdf).

Data from the 'COVID-19 repeat imaging study' has been released on a rolling basis. As of March 24, 2023, we identified N = 416 (including n = 224 COVID-19 positive case) participants from the matched case-control list (variable ID 41000 in the UKB Data Showcase), who met the following inclusion criteria of the current study: 1) no mismatch between self-reported and genetic sexes, and 2) no missing data in any of the measures used in the current study. Demographic characteristics of the present study sample are summarized in **Table 1** and consistent with study design, were comparable between COVID-19 case and control participants. We also identified COVID-19 testing date for n=219 (97.77%) of the COVID-19 cases (UKB variable ID 40100). For this group of participants, the COVID-19 testing preceded the second imaging session by 128.3±70.8 days on average (range 37-372 days). Although unfortunately, data for COVID-19 related symptomatology and vaccination status were unavailable for the current study, we identified a small subgroup of COVID-19 case participants (n=13; 5.80%) who had a record for hospital inpatient admissions (variable ID 41001 in the UKB Data Showcase). Demographic information for hospitalized vs. non-hospitalized cases is summarized in **Supplemental Table S1**.

Table 1. Demographics of the Study Sample.

	Group		Between-group Difference [a]
	COVID-19 Positive (N=224)	COVID-19 Negative (N=192)	
Sex (Female/Male)	122/102	112/80	X^2 = 0.63 (p=0.43)
Race (White/non-White)	219/5	188/4	X^2 = 0.01 (p=0.92)
Age at scan1 [b] (mean (SD [c]))	59.17 (7.03)	59.79 (7.13)	t = 0.89 (p=0.38)
Age at scan2 (mean (SD [c]))	62.2 (6.73)	62.9 (6.92)	t = 1.0 (p=0.32)
Years between two scans (mean (SD))	3.03 (1.59)	3.11 (1.62)	t = 0.52 (p=0.60)
Days between COVID-19 testing and scan2 (mean (SD))	128.3 (70.2)	NA	NA
BMI at scan1 (kg/m^2, mean (SD))	26.67 (4.44)	26.48 (4.55)	t = -0.41 (p=0.68)
BMI at scan2 (kg/m^2, mean (SD))	26.56 (4.22)	26.57 (4.83)	t = 0.04 (p=0.97)
BMI between two scans (kg/m^2, mean (SD))	-0.08 (2.12)	0.17 (1.96)	t = 1.2 (p=0.23)
Smoking frequency at scan1 (mean (SD))	0.43 (0.59)	0.41 (0.55)	t = -0.35 (p=0.73)
Smoking frequency at scan2 (mean (SD))	0.36 (0.57)	0.39 (0.54)	t = 0.59 (p=0.56)
Smoking frequency between two scans (mean (SD))	-0.06 (0.39)	-0.02 (0.18)	t = 1.07 (p=0.29)
Number of participants with diagnosed diabetes	3	1	X^2 = 0.73 (p=0.39)
Number of participants with diagnosed autoimmune/inflammatory diseases	0	0	NA

[a] Between-group differences were tested with Chi-squared test for categorical (sex and race), and Welch's Two Sample t-test for numerical (age, BMI, and smoking frequency) variables.
[b] Scan 1 and Scan 2 refer to the imaging scans prior to and following the COVID-19 testing, respectively.
[c] SD = standard deviation

Imaging Acquisition and Processing.

Diffusion Weighted Imaging (DWI) and T1-weighted structural MRI scans that were processed by the UKB Brain Imaging group (50) were used in the present study. Briefly, DWI data were acquired using a two-shell approach (b_1 = 1000 and b_2 = 2000 s/mm2) with 50 distinct diffusion-encoding directions within each shell. This multi-shell acquisition scheme is comparable to those used for the development of DBSI (42,52). In general, multi-shell diffusion sequences have advantages of reduced sensitivity to the confounding effects of in-scanner motion (59) and have been shown to improve the estimation for free water corrected measures and free water fraction (60), and the angular resolution of orientation distribution functions (61). In addition, the UKB employed EPI-based spin echo acquisitions with opposite phase encode direction to reduce image distortion while reducing acquisition time (41), further increasing signal sensitivity. The acquired DWI data were then preprocessed to correct for eddy currents, head motion, outlier slice, and gradient distortion. The preprocessed data are available for download from the UKB database. T1 structural MRI data were acquired using an in-plane acceleration sequence and preprocessed to remove the skull and corrected for gradient distortion. Further processing on the T1 images was then carried out using FreeSurfer software, which produced images, surface files, and summary outputs, all available for download from the UKB database (https://biobank.ndph.ox.ac.uk/showcase/). More information about the acquisition protocols, image processing pipeline, and derived imaging measures can be found in the UK Biobank Imaging Documentation (https://biobank.ctsu.ox.ac.uk/crystal/crystal/docs/brain_mri.pdf) and studies by Alfaro-Almagro et al. (62) and Miller et al. (41) .

Diffusion Basis Spectrum Imaging and Neuroinflammation Indices.

The DBSI technique employs a linear combination of anisotropic and isotropic tensors in describing the diffusion-weighted imaging signal, thereby improving sensitivity and specificity of estimated diffusion property (37, 42, 50). The primary DBSI neuroinflammation marker, known as the restricted (cellular) fraction (DBSI-RF), correlates with elevated cellularity and has been associated with activated microglia and astrogliosis in conditions such as multiple sclerosis (43,46,48,57,63) and Alzheimer's disease (45,52,64). DBSI hindered (extracellular) fraction (DBSI-HF), which is indicative of vasogenic edema, has also been linked to neuroinflammation (65,66) and inflammatory conditions including obesity (49,50) and Alzheimer Disease (52).

To indicate neuroinflammation levels for specific brain structures, we applied the DBSI analysis package that was developed in house using the MATLAB (42) to the DWI data and used pre-defined brain structures (i.e., regions of interest, ROIs) as masks to extract region-specific neuroinflammation indices. Specifically, we used gray matter parcellations generated by the Automatic Subcortical Segmentation (67) and Desikan-Killiany cortical atlases (68). The resulting gray matter ROIs consisted of 14 bilateral subcortical and 66 cortical parcellations, representing n = 7 and n = 33 subcortical and cortical structures, respectively. Additionally, n = 20 white matter tracts from both left and right hemispheres were extracted from a probabilistic tractography atlas (JHU-ICBM-tracts) with the lowest probability of 25% at a given brain voxel (69). We used this probability threshold to ensure that each individual white matter tract could be identified in the subject-specific diffusion images (i.e., increasing probability would result in uneven tract numbers identified at the individual level).

To extract neuroinflammation indices per individual for each of the gray and white matter ROIs, we first created individual-specific ROI masks by registering T1 structural (i.e., FreeSurfer outputs) and MNI standard diffusion images (i.e., white matter tracts) with native diffusion images. The mean DBSI-RF and DBSI-HF values across all voxels within each ROI were then calculated for each individual participant, respectively. As more than half of the entire gray matter structures (n = 21) showed a correlation less than 0.6 between the left and right

hemispheric homologues for the baseline DBSI-RF values (i.e., pre-COVID), we considered each parcellation as an independent ROI for statistical analysis (i.e., not combined across hemispheres). Similarly, all 20 white matter tracts were considered as separate ROI as the left-right correlations for all tracts from the baseline DBSI-RF values were below 0.6. We applied the same pipeline to DBSI-HF and included each individual gray matter parcellation and white matter tract as a unique ROI in the subsequent analyses involving DBSI-HF, due to low baseline correlations ($r<0.06$) between two hemispheric homologues for many gray matter structures (n=20) and white matter tracts (n=10).

Covariates

Following a prior study (20), we included genetic sex (UKB variable ID 22001), ethnicity (UKB variable ID 21000), as well as differences between pre- and post-COVID assessments in age (UKB variable ID 21003) as covariates in this study. We further included changes in body mass index (BMI; UKB variable ID 21001), in smoking status (UKB variable ID 20116), and in date (i.e., number of days; UKB variable ID 53) between two assessments to adjust for potential confounds that may contribute to the changes in neuroinflammation from pre- to post-COVID. As in this prior study (20), we also used white versus non-white for ethnicity in all models.

Statistical Analysis

We tested whether COVID-19 cases differed from controls on neuroinflammation, as indexed by DBSI-RF. Mirroring the analytic strategy of a prior study linking COVID-19 case status to brain structural changes (20), we conducted a series of linear regressions in which COVID-19 case/control status was modeled as a predictor of post-COVID regional neuroinflammation, while accounting for pre-COVID neuroinflammation and the covariates described above. Separate models were conducted for each individual ROI and false discovery rate (FDR) was applied to adjust for multiple testing within gray and white matter ROIs, separately (i.e., 40 tests for gray matter ROIs, and 20 tests for white matter ROIs). This analytic pipeline was repeated for our primary (DBSI-RF) and secondary (DBSI-HF) neuroinflammation markers, respectively.

As it is plausible that neuroinflammation may reflect a transient phenomenon resolving over time, we further conducted post-hoc analyses on data of participants whose positive COVID-19 test occurred ≤ 60 (n = 75) and ≤90 (n = 23) days prior to the neuroimaging session and conducted group comparisons of each of these two subgroups with controls separately. Furthermore, we repeated the main analyses without the restriction on the assessment time interval after excluding the data from the COVID-19 positive cases with a hospitalization record (N=13) to explore the potential impact of symptom severity on the association between neuroinflammation and COVID-19.

As changes in putative neuroinflammation within each ROI may not occur uniformly, we further explored the association between COVID-19 and whole-brain voxel-wise neuroinflammation, as indexed by DBSI-RF. To this end, we first registered all participants' DBSI-RF maps (i.e., both pre- and post-COVID maps) with the standard MNI brain template and obtained a differential map between two scans per individual (i.e., scan 2 minus scan 1; delta DBSI-map in MNI space). Using these delta maps as input, we then conducted permutation tests (permuted n = 5000) with FSL *randomise (70)* and a Threshold-Free Cluster Enhancement (TFCE) method (71) to identify delta DBSI-RF "clusters" in the brain that differ between COVID-19 negative and positive individuals (i.e., case-minus-control contrast and control-minus-case contrast), while accounting for covariates (i.e., sex, ethnicity, data acquisition interval, and changes in age, BMI, and smoking status). Categorical variables (e.g., sex, group) were dummy coded before permutation testing. These post-hoc and exploratory analyses were conducted for DBSI-RF and DBSI-HF, separately.

Results (word count = 441)

After multiple testing correction, COVID-19 was not associated with any changes in DBSI-RF values across all gray matter regions and white matter tracts. There were only a handful of nominally significant associations (i.e., uncorrected p<0.05; **Figure 1; Table 2**). Gray matter regions included the left caudal middle frontal gyrus (β = -0.14, $p_{uncorrected}$ = 0.048), superior parietal lobule (β = -0.14, $p_{uncorrected}$ = 0.047), and postcentral gyrus (β = -0.14, $p_{uncorrected}$ = 0.041), as well as the right caudate (β = 0.18, $p_{uncorrected}$ = 0.039), amygdala (β = 0.22, $p_{uncorrected}$ = 0.013), caudal anterior cingulate cortex (β=0.25, $p_{uncorrected}$ = 0.003), rostral anterior cingulate cortex (β = 0.27, $p_{uncorrected}$ = 0.003), lateral orbitofrontal cortex (β=0.19, $p_{uncorrected}$ = 0.037), and fusiform gyrus (β = 0.19, $p_{uncorrected}$ = 0.029). Only one region was nominally significant in white matter: the temporal proportion of the left superior longitudinal fasciculus (β = 0.25, $p_{uncorrected}$ = 0.008). When we repeated these analyses excluding COVID-19 case participants who had been hospitalized at the time of COVID-19 testing, results remained similar with negligibly small changes in beta values (see **Supplemental Table S2**).

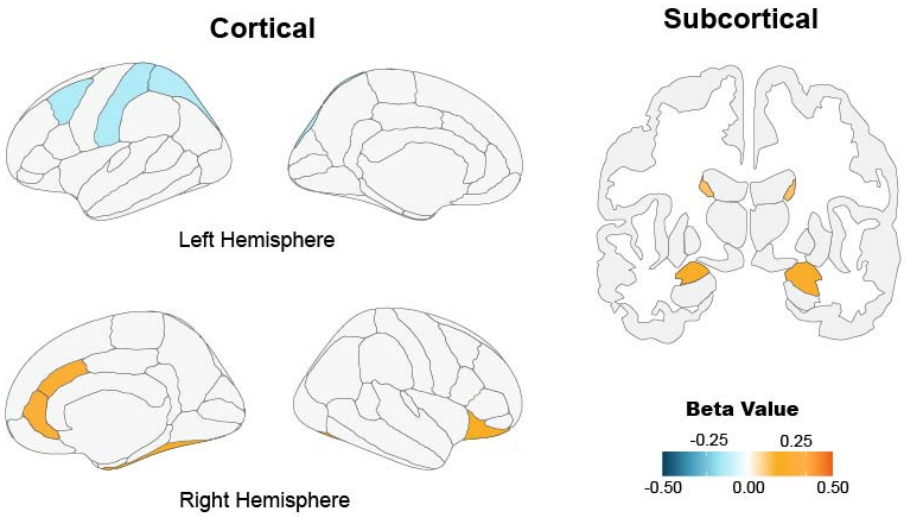

Figure 1. Gray Matter Regions with Nominal Increase in DBSI-RF ($p_{uncorrected}$<0.05).

In contrast, COVID-19 was significantly associated with DBSI-HF values in the pre- and post-central gyri in the left hemisphere, as well as the caudal proportion of the right middle frontal gyrus after FDR corrections (β's > 0.3, FDR p's = 0.03; **Figure 2**). In addition, a set of cortical regions and white matter tracts exhibited nominally significant associations, such as bilateral superior frontal gyrus, bilateral pars triangularis, and right cingulum bundle (β's > 0.15, uncorrected p's < 0.05; see full list in **Table 3**). These results remained when excluding the hospitalized participants (**Supplemental Table S3**).

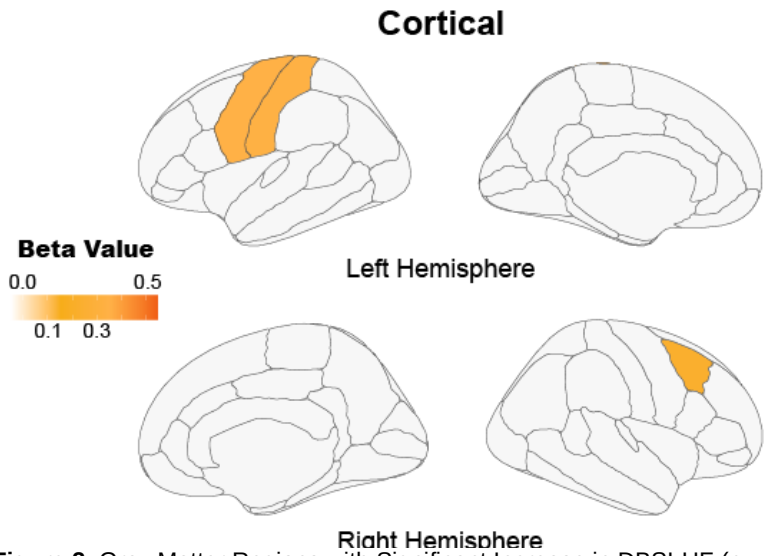

Figure 2. Gray Matter Regions with Significant Increase in DBSI-HF (p_{FDR}<0.05).

Table 2. Nominally significant between-group differences in DBSI-RF.

Brain Structure	ROI (L/R) [a]	Statistics [b]			
		B [95% CI] [c]	*t*	Uncorrected P-value	FDR corrected P-value [d]
Subcortical					
	Caudate (R)	0.18 [0.01, 0.35]	2.08	0.039	0.424
	Amygdala (R)	0.22 [0.04, 0.41]	2.49	0.013	0.356
Cortical					
	Caudal Middle Frontal (L)	-0.14 [-0.28, 0.001]	-1.99	0.048	0.424
	Postcentral (L)	-0.14 [-0.27, 0.003]	-2.05	0.041	0.424
	Superior Parietal (L)	-0.13 [-.027, 0.001]	-1.99	0.047	0.424
	Caudal Anterior Cingulate (R)	0.25 [0.05, 0.44]	2.54	0.011	0.356
	Fusiform (R)	0.19 [0.02, 0.36]	2.20	0.029	0.424
	Lateral Orbitofrontal (R)	0.19 [0.01, 0.38]	2.09	0.037	0.424
	Rostral Anterior Cingulate (R)	0.27 [0.09, 0.46]	2.94	0.003	0.279
White Matter Tracts					
	Superior Longitudinal Fasciculus (L; Temporal Part)	0.25 [0.06, 0.44]	2.66	0.008	0.165

[a] ROI = Regions of Interest; L/R = Left / Right hemisphere
[b] Group difference between the COVID-19 positive and negative participants after adjusting for the covariates.
[c] CI = Confidence Interval
[d] FDR = False Discovery Rate

Table 3. Nominally and statistically significant between-group differences in DBSI-HF.

Brain Structure	ROI (L/R) [a]	Statistics [b]			
		B [95% CI] [c]	*t*	Uncorrected P-value	FDR corrected P-value [d]
Cortical					
	Caudal Middle Frontal (L)	0.28 [0.08,0.48]	2.75	0.006	0.074
	Inferior Parietal (L)	0.20 [0.004,0.39]	2.0	0.046	0.174
	Middle Temporal (L)	0.22 [0.04,0.40]	2.34	0.02	0.145
	Paracentral (L)	0.26 [0.07,0.45]	2.74	0.006	0.074
	Pars Opercularis (L)	0.21 [0.02,0.40]	2.18	0.03	0.16
	Pars Triangularis (L)	0.25 [0.06,0.45]	2.54	0.01	0.102
	Postcentral (L)	0.32 [0.13,0.51]	3.28	0.001	**0.03***
	Precentral (L)	0.33 [0.14,0.53]	3.38	0.0008	**0.03***
	Rostral Middle Frontal (L)	0.27 [0.07,0.46]	2.68	0.008	0.077
	Superior Frontal (L)	0.28 [0.08,0.47]	2.82	0.005	0.074
	Superior Parietal (L)	0.21 [0.02,0.40]	2.12	0.03	0.160
	Supramarginal (L)	0.26 [0.08,0.45]	2.78	0.006	0.074
	Transverse Temporal	0.18 [0.01,0.35]	2.08	0.038	0.16
	Insula (L)	0.20 [0.006,0.39]	2.02	0.044	0.174
	Caudal Middle Frontal (R)	0.33 [0.13,0.52]	3.30	0.001	**0.03***
	Isthmus Cingulate (R)	0.20 [0.02,0.39]	2.16	0.03	0.16
	Pars Triangularis (R)	0.23 [0.03,0.43]	2.28	0.02	0.155
	Precentral (R)	0.21 [0.01,0.40]	2.09	0.037	0.16
	Precuneus (R)	0.20 [0.01,0.38]	2.10	0.036	0.16
	Rostral Middle Frontal (R)	0.24 [0.05,0.44]	2.41	0.016	0.13
	Superior Frontal (R)	0.22 [0.02,0.42]	2.16	0.03	0.16
White Matter Tracts					
	Cingulum (R; Anterior and Superior Portion)	0.19 [0.04,0.34]	2.54	0.011	0.138

	Superior Longitudinal Fasciculus (R; Temporal Part)	-0.21 [-0.38,-0.04]	-2.47	0.014	0.138

[a] ROI = Regions of Interest; L/R = Left / Right hemisphere
[b] Group difference between the COVID-19 positive and negative participants after adjusting for the covariates.
[c] CI = Confidence Interval
[d] FDR = False Discovery Rate
[*] Significant results after FDR corrections

Proximity of Scan to COVID-19 Diagnosis.
After accounting for multiple testing, we did not observe significant differences in either DBSI-RF or DBSI-HF values between participants whose COVID-19 positive tests were closer in time to the neuroimaging session (i.e., ≤ 60 or ≤ 90 days following COVID-19 test) and non-infected control participants. Yet, nominally higher DBSI-RF values were observed in several brain structures and tracts, including rostral anterior cingulate cortex in the right hemisphere (β's > 0.3, uncorrected p's < 0.05), which were also observed in the full sample (**Table 4**). Further, DBSI-HF values in several regions including the left pars triangularis, right cuneus cortex, and the rostral portion of the anterior cingulate cortex showed nominally significant associations with COVID-19 in both subsets across different time-windows (|β|'s > 0.2, uncorrected p's < 0.05; **Table 5**).

Whole-brain voxel-wise differences in putative neuroinflammation.
After applying threshold-free cluster enhancement (TFCE), we did not observe any clusters that reached a statistical significance (all p's>0.05) for DBSI-RF or DBSI-HF.

Table 4. Nominally significant between-group differences in DBSI-RF in potentially acute COVID-19 cases.

Brain Structure	ROI (L/R) [a]	Statistics							
		≤ 60 Days [b]				≤ 90 Days [b]			
		β [95% CI] [c]	*t*	Uncorrected P-value	FDR corrected P-value	β [95% CI] [c]	*t*	Uncorrected P-value	FDR corrected P-value [d]
Subcortical									
	Hippocampus (R)					0.27 [0.03, 0.52]	2.22	0.027	0.463
Cortical									
	Pars Triangularis (L)	-0.39 [-0.75, -0.02]	-2.11	0.036	0.597	-0.24 [-0.46, -0.02]	-2.22	0.027	0.463
	Postcentral (L)					-0.21 [-0.41, -0.02]	-2.19	0.029	0.463
	Cuneus (R)	0.37 [0.02, 0.72]	2.13	0.035	0.597	0.23 [0.01, 0.45]	2.12	0.035	0.463
	Fusiform (R)					0.28 [0.04, 0.53]	2.33	0.020	0.463
	Pericalcarine Cortex (R)	0.41 [0.02, 0.80]	2.10	0.037	0.597				
	Rostral Anterior Cingulate (R)	0.52 [0.09, 0.95]	2.40	0.011	0.597	0.32 [0.06, 0.58]	2.45	0.015	0.463
	Rostral Middle Frontal (R)	-0.41 [-0.76, 0.07]	-2.39	0.029	0.597				
White Matter Tracts									
	Superior Longitudinal Fasciculus (L; Temporal Part)					0.34 [0.07, 0.60]	2.53	0.012	0.243

[a] ROI = Regions of Interest; L/R = Left / Right hemisphere
[b] Group comparisons of COVID-19 negative individuals with COVID-19 positive individuals whose COVID-19 positive testing occurred within 60 or 90 days of their second imaging scan.
[c] CI = Confidence Interval
[d] FDR = False Discovery Rate

Table 5. Nominally significant between-group differences in DBSI-HF in potentially acute COVID-19 cases.

Brain Structure	ROI (L/R) [a]	Statistics							
		≤ 60 Days [b]				≤ 90 Days [b]			
		β [95% CI] [c]	*t*	Uncorrected P-value	FDR corrected P-value	β [95% CI] [c]	*t*	Uncorrected P-value	FDR corrected P-value [d]
Subcortical									
	Thalamus (L)					0.30 [0.09,0.50]	2.81	0.005	0.065
Cortical									
	Caudal Anterior Cingulate (L)					0.28 [0.02,0.54]	2.07	0.04	0.177
	Cuneus (L)					0.28 [0.02, 0.53]	2.15	0.033	0.162
	Inferior Parietal (L)					0.34 [0.07,0.60]	2.46	0.01	0.13
	Middle Temporal (L)					0.41 [0.15,0.67]	3.12	0.002	0.065
	Postcentral (L)					0.38 [0.12,0.65]	2.84	0.005	0.065
	Precentral (L)					0.39 [0.12,0.66]	2.84	0.005	0.065
	Rostral Middle Frontal (L)					0.33 [0.06,0.60]	2.37	0.02	0.143
	Superior Frontal (L)					0.28 [0.01,0.55]	2.07	0.04	0.177
	Superior Parietal (L)					0.31 [0.04,0.58]	2.24	0.026	0.149
	Supramarginal (L)					0.39 [0.14,0.64]	3.01	0.003	0.065
	Transverse Temporal (L)					0.25 [0.02,0.48]	2.17	0.03	0.162
	Caudal Middle Frontal (R)					0.39 [0.13,0.66]	2.87	0.004	0.065
	Cuneus (R)	0.43 [0.05, 0.86]	1.98	0.05	0.823	0.37 [0.11,0.63]	2.79	0.006	0.065
	Isthmus Cingulate (R)					0.30 [0.04,0.55]	2.30	0.02	0.143
	Precentral (R)					0.31 [0.05,0.58]	2.33	0.02	0.143

	Precuneus (R)					0.33 [0.08,0.59]	2.55	0.01	0.114
	Superior Parietal (R)					0.30 [0.04,0.56]	2.28	0.02	0.143
White Matter Tracts									
	Superior Longitudinal Fasciculus (L; Temporal Part)					0.34 [0.07, 0.60]	2.53	0.012	0.243
	Cingulum (R; Anterior and Superior Portion)	-0.44 [-0.86,-0.02]	-2.05	0.04	0.412	-0.27	-2.06	0.04	0.27
	Inferior Frontooccipital Fasciculus (R)	-0.41 [-0.79,-0.03]	-2.12	0.04	0.412				
	Inferior Longitudinal Fasciculus (R)					-0.26 [-0.48,-0.04]	-2.28	0.02	0.237
	Superior Longitudinal Fasciculus (R; Temporal Part)					-0.32 [-0.57,-0.08]	-2.63	0.009	0.183

[a] ROI = Regions of Interest; L/R = Left / Right hemisphere
[b] Group comparisons of COVID-19 negative individuals with COVID-19 positive individuals whose COVID-19 positive testing occurred within 60 or 90 days of their second imaging scan.
[c] CI = Confidence Interval
[d] FDR = False Discovery Rate

Discussion (word count = 1,770)

In this study we examined whether COVID-19 case status is associated with changes in neuroinflammation, as indexed by DBSI-RF (cellularity) and DBSI-HF (vasogenic edema), using a unique UKB prospective case-control cohort (n=224 cases; n=129 controls) that was scanned prior to and following COVID-19 testing. Contrary to our hypotheses and prior studies on post-mortem brain tissue (38,56) and *in vivo* imaging of long-COVID cases (36), we found no significant association between COVID-19 status and changes in DBSI-RF after multiple testing correction. Notably, several brain regions such as the orbitofrontal cortex, anterior cingulate cortex, ventral striatum, which have demonstrated the most significant structural changes following COVID-19 (20), showed increases in DBSI-RF at nominal levels of significance among COVID-19 cases (**Table 2**). These findings were replicated in analyses focused on case participants who were scanned closer to their COVID-19 test date (≤ 60 or 90 days; **Table 4**) and when excluding n=13 hospitalized individuals (**Table S2**). However, caution is warranted in interpreting these nominal findings due to their failure to survive multiple testing correction, and the inconsistent directionality of findings across regions (e.g., reduced DBSI-RF among COVID-19 cases in the caudal middle frontal gyrus). Conversely, using DBSI-RF as a secondary measure for neuroinflammation, we observed significant associations between COVID-19 status and increased DBSI-HF values (**Table 3**). Although these findings persisted when excluding hospitalized individuals (see **Table S3**), they were no longer evident when examining COVID-19 case participants with a shorter time interval between COVID-19 testing and post-COVID imaging assessment (**Table 5**).

Together, our data suggest that the putative vasogenic edema may be more sensitive in capturing changes in neuroinflammatory processes following SARS-CoV-2 infection in our sample. Yet, it also remains possible that certain COVID-19 related neuroinflammatory processes such as neuroinflammation related to glia cell damage may be temporally constrained (e.g., functional recovery within 60-90 days after SARS-CoV-2 infection; (72–74)) and thus were resolved prior to the post-COVID scan.

Infection-induced Neuroinflammation Progression and Clinical Heterogeneity

In contrast to the null findings of our primary neuroinflammation marker, DBSI-RF, other studies suggest that the acute infection of SARS-CoV-2 induces neuroinflammation, potentially leading to long-term consequences including neurological and psychiatric syndromes (75). Current evidence indicates that inflammation in the central nervous system may occur as early as several weeks after the onset of SARS-CoV-2 infection (33–35), and last up to two years after the infection with widespread influences in the brain in individuals suffering from long-COVID (22,36). Alongside acute production of proinflammatory microglia (i.e., the most dominant immune cells in the brain) and a chronic loss of microglia (76), damages in astrocytes and oligodendrocytes were also observed in relation to COVID-19, which may undergo functional recovery 60-90 days after the infection onset, subsequently resulting in reductions of neuroinflammation (72–74). Alternatively, these glia cell damages may ultimately lead to neuronal cell death in the cerebral cortex (72,77). These findings suggest that COVID-19-related inflammatory processes may diverge depending on the assessment timing (78). DBSI-RF, being an indirect proxy of inflammation-related cellularity from either immune cell proliferation or infiltration (42,44,46,52), raises the possibility that these inflammatory processes may have subsided by the time of the second imaging scan. Although DBSI-RF holds potential to capture a wide range of inflammatory processes, it may also require future investigation to determine its sensitivity in detecting inflammatory changes induced by SARS-CoV-2 infection in the central nervous system. Interestingly, while our primary neuroinflammation marker, DBSI-RF showed no association with COVID-19, we observed significant increases in the putative marker

of vasogenic edema (i.e., DBSI-HF) for COVID-19 cases compared to non-infected controls. This result might indicate the presence of continued neuroinflammation in these case participants, consistent with the prolonged nature of neurological consequences following the resolution of acute COVID-19 illness. However, our mixed findings of DBSI markers may be influenced by the clinical heterogeneity of COVID-19 manifestations with some case participants possibly having fully recovered from the infection, while some others still experiencing some degrees of symptoms by the time of the second imaging assessment. The lack of information regarding the disease recovery and the real-time symptoms for COVID-19 positive cases adds complexity to our interpretation.

It should also be noted that the present findings were obtained after correcting for potential confounding effects of age, sex, ethnicity, BMI, smoking frequency, and data acquisition intervals. Additional factors may contribute to variations in clinical presentation and related neuroinflammation. For instance, a “two-hit” hypothesis on the link between microglial activation and COVID-19 severity suggests that predisposed conditions such as exposures to childhood trauma (i.e., first hit) may sensitize individuals’ microglia responses when facing the second immune challenge, such as COVID-19 (79). In line with this, a recent survey study has reported increased risks of developing post-infection conditions for individuals who had indicated prior-infection distress (80). Interestingly, however, psychological stress has also been linked to neuroinflammation in non-infected control participants during the COVID-19 pandemic, suggesting that neuroimmune activation may contribute to the development of symptoms not directly linked to the coronavirus SARS-CoV-2 (81). Future research may consider including stress-related factors to better understand neuroinflammation induced by SARS-CoV-2 infection and its implications.

Nominal Associations of DBSI-RF with COVID-19

A few nominally significant results (i.e., before FDR correction) in DBSI-RF values are worth mentioning in the context of prior research findings. First, the lateral orbitofrontal cortex exhibited a nominally higher level of post-COVID neuroinflammation in individuals who were tested COVID-19 positive before the second imaging assessment. This finding aligns with prior animal studies that highlighted the susceptibility of the olfactory system, including the orbitofrontal regions, to SARS-CoV-2 virus invasion, showing the olfactory bulb as the primary entry point for the virus into the brain (82), with the nasal cavity's olfactory epithelium identified as the enhanced binding site of the virus (83,84). The initial virus invasion is then followed by a rapid and trans-neuronal spread of infection throughout the brain, including structures connected with the olfactory bulb as well as structures only remotely connected with the olfactory system (82). This wide spread infection may further manifest at the structural level of the brain such that even mildly or moderately infected individuals (i.e., non-hospitalized) exhibited greater reduction in grey matter thickness and tissue contrast in the orbitofrontal cortex (20). Additionally, our results indicated that regions that are functionally connected to the piriform cortex (i.e., the primary component of the olfactory network) including the amygdala, caudate, and the anterior cingulate cortex also showed nominally higher neuroinflammation levels in COVID-19 positive individuals (**Table 2**). Interestingly, these regions were previously reported with longitudinal anatomical changes in the same UK Biobank cohort who were COVID-19 positive with mild-to-moderate symptoms (20). In addition to these gray matter structures, the COVID-19 positive individuals in our study also had higher neuroinflammation in the temporal part of the superior longitudinal fasciculus (SLF), a white matter tract mainly connects the frontal and parietal cortices and plays a crucial role in language, attention, memory, and emotion (85,86). Altered diffusion properties in SLF have been reported in post-COVID individuals who had mild to moderate acute COVID-19 (87,88), and these alterations appear to be persistent long after recovery of COVID-19 (25,87). Thus, the nominally elevated

neuroinflammation in SLF might also be indicative of this pathological process induced by COVID-19. However, as these findings did not survive FDR correction, they should be interpreted with caution.

Significant and Nominal Associations of DBSI-HF with COVID-19

While our primary measure of putative neuroinflammation-related cellularity did not exhibit significant associations with COVID-19, we observed an increased ratio of extracellular water (indicative of vasogenic edema) in COVID-19 cases compared to non-infected controls (**Table 3**). This is in line with previous observations of cerebral or brain tissue edema in patients with COVID-19 (21,89,90), Notably, heightened DBSI-HF in our study was found in primary motor and primary sensorimotor areas, which have previously shown aberrant connectivity patterns in individuals with acute SARS-CoV-2 infection (91), or six months after hospital discharge (92). Long-term changes in resting-state amplitude of low-frequency fluctuation (ALFF) were also reported for these areas in patients one year after recovery (16). Furthermore, the caudal middle frontal gyrus, exhibiting increased DBSI-HF in our study, has been linked to SARS-CoV-2-induced structural changes such as reduced cortical thickness (93). Interestingly, this COVID-19-related structural alteration within this brain region was further associated with increased inflammation markers in the cerebrospinal fluid (94). Yet, it is noteworthy that these prior findings were observed in individuals with a diverse spectrum of post-COVID sequelae (e.g., persistent fatigue and myalgia), suggesting that post-SARS-CoV-2 inflammatory processes may be symptom-dependent (95). Due to the lack of information about COVID-19 symptomatology in our study, future investigations are needed to explore the associations between COVID-19 symptoms and vasogenic edema present after SARS-CoV-2 infection.

Limitations

It is important to consider study limitations when interpreting these data. First, COVID-19 positive cases in our study were defined solely by SARS-Cov-2 testing while symptom and severity assessments, as well as vaccination status were unavailable (96). This precluded us from investigating associations between the DBSI-derived putative neuroinflammation markers and COVID-19 symptomatology. While elevated peripheral inflammation markers have been observed in individuals with SARS-Cov-2 infection and are tied to the severity of COVID-19 symptoms (89,97–99), inflammatory responses appear to regress gradually during recovery in most patients (100,101), This indicates a transient effect of inflammation that potentially is symptom dependent. It is therefore possible that our mixed findings in DBSI-RF and DBSI-HF are attributable to the study assessment schedule (i.e., second scan acquired on average 128 days post COVID-19) and lack of COVID-19 symptomatology data available to us. Future research is warranted to examine the impact of COVID-19 symptom severity on different neuroinflammatory processes following SARS-CoV-2 infection. Second, while the UK Biobank is population-based cohort, it is also self-selective (102) and predominantly White (**Table 1**), which may limit the generalizability of these findings. Third, information of COVID-19 testing date for control participants were unavailable, making it impossible to model within-subject variability in neuroinflammation changes due to differences in the time interval between COVID-19 testing and the second imaging assessment for the full study sample.

Conclusion

While no statistical association was found between COVID-19 status and DBSI-RF, a relatively large sample of case participants (n = 224) demonstrated significant increases in DBSI-HF compared to non-infected controls (n = 192). These findings are consistent with prior research showing elevated neuroinflammation in postmortem brain tissues from severe COVID-19 patients (38,77), and in long-COVID patients with persistent neurological or psychiatric

symptoms (22,36). Considering the potential impact of analysis timing on capturing distinct inflammatory responses to COVID-19 (78), our data suggest that neuroinflammation may be both time- and symptom-dependent. However, due to the lack of relevant information in our study, these findings should be interpreted with caution.

Statement of Ethics

All participants in UK Biobank study have provided their written informed consent and that the current study has been granted an exemption from requiring ethics approval by the IRB at Washington University in St. Louis. This study was conducted under the UK Biobank Application ID 47267.

Conflict of Interest Statement

The authors have no conflicts of interest to declare.

Funding Sources

WZ was supported by McDonnell Center for Systems Neuroscience at Washington University in St. Louis. AG was supported by NSF DGE-213989. TH receives funding from NIH (R01 DK126826, NS109487 and HD070855). RB receives funding from NIH (R01 AG061162, R21 AA027827, R01 DA054750, U01 DA055367). JB receives funding from the NIH (NIMH R01 MH128286) and from the McDonnell Center for Systems Neuroscience.

Author Contributions

AA and RB conceived the idea. QW and TH contributed to DBSI processing and interpretation. WZ analyzed the data and wrote the first draft of the article together with AG. JB and RB contributed to supervision. All authors contributed to the manuscript preparation.

Data Availability Statement

The UK Biobank data used in this study can be accessed by researchers upon application (https://www.ukbiobank.ac.uk/register-apply).

Reference

1. Akinbami LJ. SARS-CoV-2 Serology and Self-Reported Infection Among Adults — National Health and Nutrition Examination Survey, United States, August 2021–May 2022. MMWR Morb Mortal Wkly Rep [Internet]. 2022 [cited 2023 Jun 20];71. Available from: https://www.cdc.gov/mmwr/volumes/71/wr/mm7148a4.htm

2. Baj J, Karakuła-Juchnowicz H, Teresiński G, Buszewicz G, Ciesielka M, Sitarz R, et al. COVID-19: Specific and Non-Specific Clinical Manifestations and Symptoms: The Current State of Knowledge. J Clin Med. 2020 Jun 5;9(6):1753.

3. Ma Y, Deng J, Liu Q, Du M, Liu M, Liu J. Long-Term Consequences of COVID-19 at 6 Months and Above: A Systematic Review and Meta-Analysis. Int J Environ Res Public Health. 2022 Jun 3;19(11):6865.

4. Mehandru S, Merad M. Pathological sequelae of long-haul COVID. Nat Immunol. 2022 Feb;23(2):194–202.

5. Chasco EE, Dukes K, Jones D, Comellas AP, Hoffman RM, Garg A. Brain Fog and Fatigue following COVID-19 Infection: An Exploratory Study of Patient Experiences of Long COVID. Int J Environ Res Public Health. 2022 Nov 23;19(23):15499.

6. Premraj L, Kannapadi NV, Briggs J, Seal SM, Battaglini D, Fanning J, et al. Mid and long-term neurological and neuropsychiatric manifestations of post-COVID-19 syndrome: A meta-analysis. J Neurol Sci. 2022 Mar 15;434:120162.

7. Naseer S, Khalid S, Parveen S, Abbass K, Song H, Achim MV. COVID-19 outbreak: Impact on global economy. Front Public Health. 2022;10:1009393.

8. Cutler, David M. The Economic Cost of Long COVID: An Update [Internet]. [cited 2023 Aug 28]. Available from: https://scholar.harvard.edu/files/cutler/files/long_covid_update_7-22.pdf

9. Cutler DM. The Costs of Long COVID. JAMA Health Forum. 2022 May 12;3(5):e221809.

10. Isasi F, Naylor MD, Skorton D, Grabowski DC, Hernández S, Rice VM. Patients, Families, and Communities COVID-19 Impact Assessment: Lessons Learned and Compelling Needs. NAM Perspect. 2021:10.31478/202111c.

11. Malik P, Patel K, Pinto C, Jaiswal R, Tirupathi R, Pillai S, et al. Post-acute COVID-19 syndrome (PCS) and health-related quality of life (HRQoL)—A systematic review and meta-analysis. Journal of Medical Virology. 2022;94(1):253–62.

12. Parsons N, Outsikas A, Parish A, Clohesy R, D'Aprano F, Toomey F, et al. Modelling the Anatomic Distribution of Neurologic Events in Patients with COVID-19: A Systematic Review of MRI Findings. AJNR Am J Neuroradiol. 2021 Jul;42(7):1190–5.

13. Lu Y, Li X, Geng D, Mei N, Wu PY, Huang CC, et al. Cerebral Micro-Structural Changes in COVID-19 Patients - An MRI-based 3-month Follow-up Study. EClinicalMedicine. 2020 Aug;25:100484.

14. Kumar PR, Shilpa B, Jha RK. Brain disorders: Impact of mild SARS-CoV-2 may shrink several parts of the brain. Neurosci Biobehav Rev. 2023 Jun;149:105150.

15. Radmanesh A, Derman A, Lui YW, Raz E, Loh JP, Hagiwara M, et al. COVID-19–associated Diffuse Leukoencephalopathy and Microhemorrhages. Radiology. 2020 Oct;297(1):E223–7.

16. Du YY, Zhao W, Zhou XL, Zeng M, Yang DH, Xie XZ, et al. Survivors of COVID-19 exhibit altered amplitudes of low frequency fluctuation in the brain: a resting-state functional magnetic resonance imaging study at 1-year follow-up. Neural Regeneration Research. 2022 Jul;17(7):1576.

17. Hosp JA, Dressing A, Blazhenets G, Bormann T, Rau A, Schwabenland M, et al. Cognitive impairment and altered cerebral glucose metabolism in the subacute stage of COVID-19. Brain. 2021 May 7;144(4):1263–76.

18. Guedj E, Million M, Dudouet P, Tissot-Dupont H, Bregeon F, Cammilleri S, et al. 18F-FDG brain PET hypometabolism in post-SARS-CoV-2 infection: substrate for persistent/delayed disorders? Eur J Nucl Med Mol Imaging. 2021 Feb;48(2):592–5.

19. Churchill NW, Roudaia E, Chen JJ, Gilboa A, Sekuler A, Ji X, et al. Effects of post-acute COVID-19 syndrome on the functional brain networks of non-hospitalized individuals. Front Neurol. 2023;14:1136408.

20. Douaud G, Lee S, Alfaro-Almagro F, Arthofer C, Wang C, McCarthy P, et al. SARS-CoV-2 is associated with changes in brain structure in UK Biobank. Nature. 2022;604(7907):697–707.

21. Rau A, Schroeter N, Blazhenets G, Dressing A, Walter LI, Kellner E, et al. Widespread white matter oedema in subacute COVID-19 patients with neurological symptoms. Brain. 2022 Sep 14;145(9):3203–13.

22. Braga J, Lepra M, Kish SJ, Rusjan PabloM, Nasser Z, Verhoeff N, et al. Neuroinflammation After COVID-19 With Persistent Depressive and Cognitive Symptoms. JAMA Psychiatry [Internet]. 2023 May 31 [cited 2023 Jul 5]; Available from: https://doi.org/10.1001/jamapsychiatry.2023.1321

23. Mazza MG, Palladini M, De Lorenzo R, Magnaghi C, Poletti S, Furlan R, et al. Persistent psychopathology and neurocognitive impairment in COVID-19 survivors: Effect of inflammatory biomarkers at three-month follow-up. Brain Behav Immun. 2021 May;94:138–47.

24. Huang S, Zhou Z, Yang D, Zhao W, Zeng M, Xie X, et al. Persistent white matter changes in recovered COVID-19 patients at the 1-year follow-up. Brain. 2021 Dec 16;145(5):1830–8.

25. Huang S, Zhou X, Zhao W, Du Y, Yang D, Huang Y, et al. Dynamic white matter changes in recovered COVID-19 patients: a two-year follow-up study. Theranostics. 2023 Jan 1;13(2):724–35.

26. Merad M, Martin JC. Pathological inflammation in patients with COVID-19: a key role for monocytes and macrophages. Nat Rev Immunol. 2020 Jun;20(6):355–62.

27. Darif D, Hammi I, Kihel A, El Idrissi Saik I, Guessous F, Akarid K. The pro-inflammatory cytokines in COVID-19 pathogenesis: What goes wrong? Microb Pathog. 2021 Apr;153:104799.

28. Rabaan AA, Al-Ahmed SH, Muhammad J, Khan A, Sule AA, Tirupathi R, et al. Role of Inflammatory Cytokines in COVID-19 Patients: A Review on Molecular Mechanisms, Immune Functions, Immunopathology and Immunomodulatory Drugs to Counter Cytokine Storm. Vaccines (Basel). 2021 Apr 29;9(5):436.

29. Channappanavar R, Perlman S. Pathogenic human coronavirus infections: causes and consequences of cytokine storm and immunopathology. Semin Immunopathol. 2017;39(5):529–39.

30. Ragab D, Salah Eldin H, Taeimah M, Khattab R, Salem R. The COVID-19 Cytokine Storm; What We Know So Far. Frontiers in Immunology [Internet]. 2020 [cited 2023 Jun 24];11. Available from: https://www.frontiersin.org/articles/10.3389/fimmu.2020.01446

31. Meinhardt J, Radke J, Dittmayer C, Franz J, Thomas C, Mothes R, et al. Olfactory transmucosal SARS-CoV-2 invasion as a port of central nervous system entry in individuals with COVID-19. Nat Neurosci. 2021 Feb;24(2):168–75.

32. Krasemann S, Haferkamp U, Pfefferle S, Woo MS, Heinrich F, Schweizer M, et al. The blood-brain barrier is dysregulated in COVID-19 and serves as a CNS entry route for SARS-CoV-2. Stem Cell Reports. 2022 Feb 8;17(2):307–20.

33. Kanberg N, Simrén J, Edén A, Andersson LM, Nilsson S, Ashton NJ, et al. Neurochemical signs of astrocytic and neuronal injury in acute COVID-19 normalizes during long-term follow-up. EBioMedicine. 2021 Jul 29;70:103512.

34. Vanderheiden A, Klein RS. Neuroinflammation and COVID-19. Current Opinion in Neurobiology. 2022 Oct 1;76:102608.

35. Farhadian S, Glick LR, Vogels CBF, Thomas J, Chiarella J, Casanovas-Massana A, et al. Acute encephalopathy with elevated CSF inflammatory markers as the initial presentation of COVID-19. BMC Neurology. 2020 Jun 18;20(1):248.

36. Visser D, Golla SSV, Verfaillie SCJ, Coomans EM, Rikken RM, Giessen EM van de, et al. Long COVID is associated with extensive in-vivo neuroinflammation on [18F]DPA-714 PET [Internet]. medRxiv; 2022 [cited 2023 Jun 20]. p. 2022.06.02.22275916. Available from: https://www.medrxiv.org/content/10.1101/2022.06.02.22275916v1

37. Frere JJ, Serafini RA, Pryce KD, Zazhytska M, Oishi K, Golynker I, et al. SARS-CoV-2 infection in hamsters and humans results in lasting and unique systemic perturbations after recovery. Science Translational Medicine. 2022 Jun 7;14(664):eabq3059.

38. Yang AC, Kern F, Losada PM, Agam MR, Maat CA, Schmartz GP, et al. Dysregulation of brain and choroid plexus cell types in severe COVID-19. Nature. 2021 Jul;595(7868):565–71.

39. Philippens IHCHM, Böszörményi KP, Wubben JA, Fagrouch ZC, Driel N van, Mayenburg AQ, et al. SARS-CoV-2 causes brain inflammation and induces Lewy body formation in macaques [Internet]. bioRxiv; 2021 [cited 2023 Jun 20]. p. 2021.02.23.432474. Available from: https://www.biorxiv.org/content/10.1101/2021.02.23.432474v2

40. Wischmann J, Bartos LM, Brendel M, Albert NL, Forbrig R, Straube A, et al. Translocator protein (TSPO)-PET as diagnostic and monitoring tool in COVID-19 related MRI-negative brainstem encephalitis: a case report. J Neurol. 2023;270(6):2853–6.

41. Miller KL, Alfaro-Almagro F, Bangerter NK, Thomas DL, Yacoub E, Xu J, et al. Multimodal population brain imaging in the UK Biobank prospective epidemiological study. Nat Neurosci. 2016 Nov;19(11):1523–36.

42. Wang Y, Wang Q, Haldar JP, Yeh FC, Xie M, Sun P, et al. Quantification of increased cellularity during inflammatory demyelination. Brain. 2011 Dec 1;134(12):3590–601.

43. Cross AH, Song SK. "A new imaging modality to non-invasively assess multiple sclerosis pathology." J Neuroimmunol. 2017 Mar 15;304:81–5.

44. Wang X, Cusick MF, Wang Y, Sun P, Libbey JE, Trinkaus K, et al. Diffusion basis spectrum imaging detects and distinguishes coexisting subclinical inflammation, demyelination and axonal injury in experimental autoimmune encephalomyelitis mice. NMR Biomed. 2014 Jul;27(7):843–52.

45. Wu W, Wang Q, Sun Z, Flores S, Hobbs DA, Franklin EE, et al. Initial Correlation Analysis of Diffusion Basis Spectrum Imaging of Alzheimer's Brain and Quantitative Histology. Alzheimer's & Dementia. 2022;18(S6):e064265.

46. Wang Y, Sun P, Wang Q, Trinkaus K, Schmidt RE, Naismith RT, et al. Differentiation and quantification of inflammation, demyelination and axon injury or loss in multiple sclerosis. Brain. 2015 May;138(Pt 5):1223–38.

47. Shirani A, Sun P, Schmidt RE, Trinkaus K, Naismith RT, Song SK, et al. Histopathological correlation of diffusion basis spectrum imaging metrics of a biopsy-proven inflammatory demyelinating brain lesion: A brief report. Mult Scler. 2019 Dec;25(14):1937–41.

48. Ye Z, George A, Wu AT, Niu X, Lin J, Adusumilli G, et al. Deep learning with diffusion basis spectrum imaging for classification of multiple sclerosis lesions. Ann Clin Transl Neurol. 2020 May;7(5):695–706.

49. Ly M, Raji CA, Yu GZ, Wang Q, Wang Y, Schindler SE, et al. Obesity and White Matter Neuroinflammation Related Edema in Alzheimer's Disease Dementia Biomarker Negative Cognitively Normal Individuals. J Alzheimers Dis. 2021;79(4):1801–11.

50. Samara A, Murphy T, Strain J, Rutlin J, Sun P, Neyman O, et al. Neuroinflammation and White Matter Alterations in Obesity Assessed by Diffusion Basis Spectrum Imaging. Frontiers in Human Neuroscience [Internet]. 2020 [cited 2022 Nov 1];13. Available from: https://www.frontiersin.org/articles/10.3389/fnhum.2019.00464

51. Strain JF, Burdo TH, Song SK, Sun P, El-Ghazzawy O, Nelson B, et al. Diffusion Basis Spectrum Imaging Detects Ongoing Brain Inflammation in Virologically Well Controlled HIV+ Patients. J Acquir Immune Defic Syndr. 2017 Dec 1;76(4):423–30.

52. Wang Q, Wang Y, Liu J, Sutphen CL, Cruchaga C, Blazey T, et al. Quantification of white matter cellularity and damage in preclinical and early symptomatic Alzheimer's disease. Neuroimage Clin. 2019;22:101767.

53. Zhang W, Rutlin J, Eisenstein SA, Wang Y, Barch D, Hershey T, et al. Neuroinflammation in the amygdala is associated with recent depressive symptoms. Biological Psychiatry: Cognitive Neuroscience and Neuroimaging [Internet]. 2023 May 9 [cited 2023 Jun 20]; Available from: https://www.sciencedirect.com/science/article/pii/S2451902223001192

54. Vavasour I, Sun P, Graf C, Yik J, Kolind S, Li D, et al. Characterisation of multiple sclerosis neuroinflammation and neurodegeneration with relaxation and diffusion basis spectrum imaging. Mult Scler. 2022 Mar;28(3):418–28.

55. Zhan J, Lin TH, Libbey JE, Sun P, Ye Z, Song C, et al. Diffusion Basis Spectrum and Diffusion Tensor Imaging Detect Hippocampal Inflammation and Dendritic Injury in a Virus-Induced Mouse Model of Epilepsy. Front Neurosci. 2018;12:77.

56. Schwabenland M, Salié H, Tanevski J, Killmer S, Lago MS, Schlaak AE, et al. Deep spatial profiling of human COVID-19 brains reveals neuroinflammation with distinct microanatomical microglia-T-cell interactions. Immunity. 2021 Jul 13;54(7):1594-1610.e11.

57. Shirani A, Sun P, Trinkaus K, Perantie DC, George A, Naismith RT, et al. Diffusion basis spectrum imaging for identifying pathologies in MS subtypes. Ann Clin Transl Neurol. 2019 Nov;6(11):2323–7.

58. Sudlow C, Gallacher J, Allen N, Beral V, Burton P, Danesh J, et al. UK Biobank: An Open Access Resource for Identifying the Causes of a Wide Range of Complex Diseases of Middle and Old Age. PLOS Medicine. 2015 Mar 31;12(3):e1001779.

59. Pines AR, Cieslak M, Larsen B, Baum GL, Cook PA, Adebimpe A, et al. Leveraging multi-shell diffusion for studies of brain development in youth and young adulthood. Dev Cogn Neurosci. 2020 Apr 22;43:100788.

60. Pasternak O, Shenton ME, Westin CF. Estimation of Extracellular Volume from Regularized Multi-Shell Diffusion MRI. Med Image Comput Comput Assist Interv. 2012;15(0 2):305–12.

61. Jeurissen B, Tournier JD, Dhollander T, Connelly A, Sijbers J. Multi-tissue constrained spherical deconvolution for improved analysis of multi-shell diffusion MRI data. Neuroimage. 2014 Dec;103:411–26.

62. Alfaro-Almagro F, Jenkinson M, Bangerter NK, Andersson JLR, Griffanti L, Douaud G, et al. Image processing and Quality Control for the first 10,000 brain imaging datasets from UK Biobank. NeuroImage. 2018 Feb 1;166:400–24.

63. Sun P, George A, Perantie DC, Trinkaus K, Ye Z, Naismith RT, et al. Diffusion basis spectrum imaging provides insights into MS pathology. Neurology - Neuroimmunology Neuroinflammation [Internet]. 2020 Mar 1 [cited 2022 Nov 1];7(2). Available from: https://nn.neurology.org/content/7/2/e655

64. Sun Z, Wu W, Xu H, Flores S, Hobbs DA, Perrin RJ, et al. Imaging and quantifying microglial activation in vivo and ex vivo using diffusion MRI – with validation by immunohistochemistry. In ALZ; 2023 [cited 2023 Sep 6]. Available from: https://alz.confex.com/alz/2023/meetingapp.cgi/Paper/79302

65. Stamatovic SM, Dimitrijevic OB, Keep RF, Andjelkovic AV. Inflammation and brain edema: new insights into the role of chemokines and their receptors. Acta Neurochir Suppl. 2006;96:444–50.

66. Dalby T, Wohl E, Dinsmore M, Unger Z, Chowdhury T, Venkatraghavan L. Pathophysiology of Cerebral Edema—A Comprehensive Review. J Neuroanaesth Crit Care. 2021 Sep;08(3):163–72.

67. Fischl B, Salat DH, Busa E, Albert M, Dieterich M, Haselgrove C, et al. Whole Brain Segmentation: Automated Labeling of Neuroanatomical Structures in the Human Brain. Neuron. 2002 Jan 31;33(3):341–55.

68. Desikan RS, Ségonne F, Fischl B, Quinn BT, Dickerson BC, Blacker D, et al. An automated labeling system for subdividing the human cerebral cortex on MRI scans into gyral based regions of interest. Neuroimage. 2006 Jul 1;31(3):968–80.

69. Mazziotta J, Toga A, Evans A, Fox P, Lancaster J, Zilles K, et al. A probabilistic atlas and reference system for the human brain: International Consortium for Brain Mapping (ICBM). Philos Trans R Soc Lond B Biol Sci. 2001 Aug 29;356(1412):1293–322.

70. Winkler AM, Ridgway GR, Webster MA, Smith SM, Nichols TE. Permutation inference for the general linear model. Neuroimage. 2014 May 15;92(100):381–97.

71. Smith SM, Nichols TE. Threshold-free cluster enhancement: addressing problems of smoothing, threshold dependence and localisation in cluster inference. Neuroimage. 2009 Jan 1;44(1):83–98.

72. Plantone D, Locci S, Bergantini L, Manco C, Cortese R, Meocci M, et al. Brain neuronal and glial damage during acute COVID-19 infection in absence of clinical neurological manifestations. J Neurol Neurosurg Psychiatry. 2022 Dec 1;93(12):1343–8.

73. Steardo L, Steardo L, Scuderi C. Astrocytes and the Psychiatric Sequelae of COVID-19: What We Learned from the Pandemic. Neurochem Res. 2023 Apr;48(4):1015–25.

74. Monje M, Iwasaki A. The neurobiology of long COVID. Neuron. 2022 Nov 2;110(21):3484–96.

75. Spudich S, Nath A. Nervous system consequences of COVID-19. Science. 2022 Jan 21;375(6578):267–9.

76. Jeong GU, Lyu J, Kim KD, Chung YC, Yoon GY, Lee S, et al. SARS-CoV-2 Infection of Microglia Elicits Proinflammatory Activation and Apoptotic Cell Death. Microbiol Spectr. 2022 Jun 29;10(3):e0109122.

77. Boroujeni ME, Simani L, Bluyssen HAR, Samadikhah HR, Zamanlui Benisi S, Hassani S, et al. Inflammatory Response Leads to Neuronal Death in Human Post-Mortem Cerebral Cortex in Patients with COVID-19. ACS Chem Neurosci. 2021 Jun 16;12(12):2143–50.

78. Liu C, Martins AJ, Lau WW, Rachmaninoff N, Chen J, Imberti L, et al. Time-resolved systems immunology reveals a late juncture linked to fatal COVID-19. Cell. 2021 Apr 1;184(7):1836-1857.e22.

79. Bouayed J, Bohn T. The link between microglia and the severity of COVID-19: The “two-hit” hypothesis. J Med Virol. 2021 Jul;93(7):4111–3.

80. Wang S, Quan L, Chavarro JE, Slopen N, Kubzansky LD, Koenen KC, et al. Associations of Depression, Anxiety, Worry, Perceived Stress, and Loneliness Prior to Infection With Risk of Post–COVID-19 Conditions. JAMA Psychiatry. 2022 Nov 1;79(11):1081–91.

81. Brusaferri L, Alshelh Z, Martins D, Kim M, Weerasekera A, Housman H, et al. The pandemic brain: Neuroinflammation in non-infected individuals during the COVID-19 pandemic. Brain Behav Immun. 2022 May;102:89–97.

82. Netland J, Meyerholz DK, Moore S, Cassell M, Perlman S. Severe acute respiratory syndrome coronavirus infection causes neuronal death in the absence of encephalitis in mice transgenic for human ACE2. J Virol. 2008 Aug;82(15):7264–75.

83. Butowt R, Bilinska K. SARS-CoV-2: Olfaction, Brain Infection, and the Urgent Need for Clinical Samples Allowing Earlier Virus Detection. ACS Chem Neurosci. 2020 May 6;11(9):1200–3.

84. Brann DH, Tsukahara T, Weinreb C, Lipovsek M, Van den Berge K, Gong B, et al. Non-neuronal expression of SARS-CoV-2 entry genes in the olfactory system suggests mechanisms underlying COVID-19-associated anosmia. Sci Adv. 2020 Jul 31;6(31):eabc5801.

85. Janelle F, Iorio-Morin C, D'amour S, Fortin D. Superior Longitudinal Fasciculus: A Review of the Anatomical Descriptions With Functional Correlates. Frontiers in Neurology [Internet]. 2022 [cited 2023 Jun 26];13. Available from: https://www.frontiersin.org/articles/10.3389/fneur.2022.794618

86. Wang X, Pathak S, Stefaneanu L, Yeh FC, Li S, Fernandez-Miranda JC. Subcomponents and connectivity of the superior longitudinal fasciculus in the human brain. Brain Struct Funct. 2016 May 1;221(4):2075–92.

87. Petersen M, Nägele FL, Mayer C, Schell M, Petersen E, Kühn S, et al. Brain imaging and neuropsychological assessment of individuals recovered from a mild to moderate SARS-CoV-2 infection. Proc Natl Acad Sci U S A. 2023 May 30;120(22):e2217232120.

88. Bispo DD de C, Brandão PR de P, Pereira DA, Maluf FB, Dias BA, Paranhos HR, et al. Brain microstructural changes and fatigue after COVID-19. Front Neurol. 2022 Nov 10;13:1029302.

89. Huang C, Wang Y, Li X, Ren L, Zhao J, Hu Y, et al. Clinical features of patients infected with 2019 novel coronavirus in Wuhan, China. The Lancet. 2020 Feb 15;395(10223):497–506.

90. Soltani Zangbar H, Gorji A, Ghadiri T. A Review on the Neurological Manifestations of COVID-19 Infection: a Mechanistic View. Mol Neurobiol. 2021 Feb 1;58(2):536–49.

91. Kafali HY, Dasgin H, Sahin D, Sozan SS, Oguz KK, Mutlu M, et al. The effect of SARS-CoV-2 virus on resting-state functional connectivity during adolescence: Investigating brain correlates of psychotic-like experiences and SARS-CoV-2 related inflammation response. Psychiatry Research: Neuroimaging. 2023 Nov 5;111746.

92. Fu Z, Tu Y, Calhoun VD, Zhang Y, Zhao Q, Chen J, et al. Dynamic functional network connectivity associated with post-traumatic stress symptoms in COVID-19 survivors. Neurobiology of Stress. 2021 Nov 1;15:100377.

93. Zhou S, Wei T, Liu X, Liu Y, Song W, Que X, et al. Causal effects of COVID-19 on structural changes in specific brain regions: a Mendelian randomization study. BMC Med. 2023 Jul 19;21(1):261.

94. Sanabria-Diaz G, Etter MM, Melie-Garcia L, Lieb JM, Psychogios MN, Hutter G, et al. Brain cortical alterations in COVID-19 patients with neurological symptoms. Front Neurosci. 2022 Oct 20;16:992165.

95. VanElzakker MB, Bues HF, Brusaferri L, Kim M, Saadi D, Ratai EM, et al. Neuroinflammation in post-acute sequelae of COVID-19 (PASC) as assessed by [11C]PBR28 PET correlates with vascular disease measures. bioRxiv. 2023 Oct 20;2023.10.19.563117.

96. Ssentongo P, Ssentongo AE, Voleti N, Groff D, Sun A, Ba DM, et al. SARS-CoV-2 vaccine effectiveness against infection, symptomatic and severe COVID-19: a systematic review and meta-analysis. BMC Infectious Diseases. 2022 May 7;22(1):439.

97. Sidhwani SK, Mirza T, Khatoon A, Shaikh F, Khan R, Shaikh OA, et al. Inflammatory Markers and COVID-19 Disease Progression. J Infect Public Health [Internet]. 2023 Jun 26 [cited 2023 Sep 14]; Available from: https://www.ncbi.nlm.nih.gov/pmc/articles/PMC10290960/

98. Xiao LN, Ran X, Zhong YX, Li SS. Clinical value of blood markers to assess the severity of coronavirus disease 2019. BMC Infectious Diseases. 2021 Sep 6;21(1):921.

99. Mahat RK, Panda S, Rathore V, Swain S, Yadav L, Sah SP. The dynamics of inflammatory markers in coronavirus disease-2019 (COVID-19) patients: A systematic review and meta-analysis. Clinical Epidemiology and Global Health. 2021 Jul 1;11:100727.

100. Mohandas S, Jagannathan P, Henrich TJ, Sherif ZA, Bime C, Quinlan E, et al. Immune mechanisms underlying COVID-19 pathology and post-acute sequelae of SARS-CoV-2 infection (PASC). Iqbal J, Zaidi M, editors. eLife. 2023 May 26;12:e86014.

101. Woodruff MC, Nguyen DC, Faliti CE, Saini AS, Lee FEH, Sanz I. Response under pressure: deploying emerging technologies to understand B-cell-mediated immunity in COVID-19. Nat Methods. 2022 Apr;19(4):387–91.

102. Fry A, Littlejohns TJ, Sudlow C, Doherty N, Adamska L, Sprosen T, et al. Comparison of Sociodemographic and Health-Related Characteristics of UK Biobank Participants With Those of the General Population. Am J Epidemiol. 2017 Nov 1;186(9):1026–34.